Multiobjective Optimization Strategies for Linear Gradient Chromatography

Deepak Nagrath, B. Wayne Bequette, and S. M. Cramer
Howard P. Isermann Dept. of Chemical Engineering, Rensselaer Polytechnic Institute, Troy, NY 12180

Achille Messac
Dept. of Mechanical, Aeronautical, and Nuclear Engineering, Rensselaer Polytechnic Institute, Troy, NY 12180

DOI 10.1002/aic.10459
Published online in Wiley InterScience (www.interscience.wiley.com).

The increase in the scale of preparative chromatographic processes for biopharmaceutical applications now necessitates the development of effective optimization strategies for large-scale processes in a manufacturing setting. The current state of the art for optimization of preparative chromatography has been limited to single objective functions. Further, there is a lack of understanding of when to use a particular objective, and how to combine and/or prioritize mutually competing objectives to achieve a true optimal solution. In this paper, these limitations are addressed by using a physical programming–based multiobjective optimization (MO) strategy. A set of Pareto solutions are first generated for model protein separations for both bi-objective (production rate and yield) and tri-objective (production rate, yield, and product pool concentration) scenarios. These Pareto frontiers are used to visualize the Pareto optimal surface for different components with various purity constraints and provide a qualitative framework to evaluate the optimal solutions. A physical programming–based multiobjective framework is then used for the quantitative evaluation of the optimal solutions for tertiary protein mixtures. This enables the interpretation of results for different sets of hierarchy and priority values assigned to the objective functions and constraints for the chromatographic processes. This novel multiobjective optimization approach computes the tradeoffs between the conflicting design objectives and helps in choosing an operating condition from infinite feasible optimal solutions. The combined quantitative and visualization framework presented in this paper sets the stage for the development of true optimal solutions for complex nonlinear preparative separations. © 2005 American Institute of Chemical Engineers *AIChE J,* 51: 511–525, 2005

Introduction

The need for the development of effective optimization strategies for large-scale chromatographic processes is becoming more pressing as the scale of biopharmaceutical applications continues to increase. The optimization of preparative chromatography has commonly been carried out using several different optimization strategies. For typical preparative chromatographic applications, various objectives have been used for the formulation of the optimization problem (Table 1). Although a wide variety of objectives have been used, the most common objective function to date has been the *production rate*, which is defined as the amount of product produced at a given level of purity per unit time, per unit volume of stationary phase material. Natarajan et al. (2000a) optimized the production rate using yield as a constraint. Although this

Correspondence concerning this article should be addressed to S. M. Carmer at crames@rpi.edu.
Current address of D. Nagrath: Center for Engineering in Medicine/Surgical Services, Massachusetts General Hospital, Harvard Medical School, Shriners Burns Hospital for Children, 51 Blossom Street, Boston, MA 02114; E-mail: dnagrath@hms.harvard.edu

Table 1. Various Objectives Used for Preparative Chromatography

Objectives	Desirability	References
Production rate	Maximization	Natarajan et al. (2000), Gallant et al. (1996), Felinger and Guiochon (1992), Golshan-Shirazi and Guiochon (1991), Janedra et al. (1998)
Yield	Greater than, fall in a particular range	Jandera (1998)
Production rate times yield	Maximization	Felinger and Guiochon (1996)
Purity	Greater than	Many sources
Solubility	Less than	Gallant et al. (1996), Natarajan et al. (2002)
Production cost	Minimization	Felinger and Guiochon (1994)
Efficiency	Maximization	Golshan-Shirazi and Guiochon (1990)
Specific production rate	Maximization	Felinger et al. (1993)
Column design parameters (length and particle diameter)	Minimization	Felinger and Guiochon (1992)
Resolution optimization factor	Maximization	Luo and Hsu (1997)

method improved the production rate and satisfied the yield as a hard constraint, it provides minimal flexibility to those who want to use yield as a soft metric while simultaneously satisfying several other lower or higher priority objectives. Felinger and Guiochon (1996) suggested using the product of production rate and yield as an alternative objective function. Even though this approach tended to improve the yield, it did so at the cost of significant reductions in the production rate.

In preparative scale chromatographic processes, there are often several competing objectives (such as production rate, yield, product pool concentration, and economics), which require a trade-off to ensure a satisfactory design. Further, in these problems it will be unlikely that the same values of design variables (flow rate, feed load, and salt concentration) will simultaneously result in the best possible values for all the objectives. The currently available strategies for optimization of these systems do not readily lead to truly desired solutions because they are either based on a single-objective function and/or are suited for a single product optimization. Moreover, there is a lack of understanding of when to use a particular objective and how to combine and/or prioritize these mutually competing objectives to achieve a true optimal solution.

Multiobjective optimization (MO) is a systematic method for dealing with competing objectives and performing these trade-offs (Hwang et al., 1980). MO methods can be classified into four categories:

(1) The minmax formulation (Tseng and Lu, 1990) is one in which the designer does not provide any preferences and directly minimizes the overall maximum value.

(2) Weighted sum, goal programming, physical programming, and lexicographic approaches—methods in which the designer provides preference information a priori (Messac, 1996; Tamiz et al., 1988).

(3) Weighted sum, e-constraint, physical programming, and others—methods that are based on designers' a posteriori information on the preferences pertaining to the objectives (Hollingdale, 1978; Ko and Moon, 2002).

(4) Interactive methods, which rely on progressive articulation of preference information (Benayoun et al., 1971; Messac, 1996).

Although multiobjective optimization has been used for numerous applications (Benayoun et al., 1971; Clark and Westerberg, 1983; Messac, 1996), there has thus far been no effort to investigate its application for preparative chromatographic processes.

The multiobjective optimization approach used in the current work is unique in that it uses a *physical programming method*, which enables the designer to formulate the product optimization problem in terms of physically meaningful terms and parameters. Physical programming provides a simple and flexible method for formulating and visualizing design optimization problems (Messac, 1996; Messac and Chen, 2000). In physical programming, the designer specifies ranges of different degrees of desirability (such as desirable, tolerable, undesirable, etc.) for each design objective, rather than physically meaningless weights for each objective. Physical programming provides a powerful tool for resolving trade-offs during the optimization and eliminates the need to find weights for each objective or for the scaling of the objectives, so that no objective numerically dominates. The physical programming (PP) approach uses both design objectives (that is, *soft metrics*) and *hard* constraints. It provides an optimal solution based on the preferences specified for *soft metrics*.

In the current work, we have formulated the optimization problem for linear gradient chromatography within a multiobjective framework using a twofold approach to assess the sensitivity and geometry of the optimal region and to determine the optimal results using various preferences and/or prioritization of objectives. This work is carried out with simulation results for binary and tertiary protein mixtures for proof of concept. A set of Pareto solutions is first generated for model protein separations using a novel normalized constraint method (Ismail and Messac, 2002). These Pareto frontiers are used to visualize the Pareto optimal surface for different components with various purity constraints and provide a qualitative framework to evaluate the various optimization scenarios for a linear gradient chromatography. A PP-based multiobjective framework is then used for the quantitative evaluation of the optimal linear gradient conditions for both binary and tertiary protein feed mixtures. This enables the interpretation of results for different sets of hierarchy and priority values assigned to the objective functions and constraints for the chromatographic processes. The presented approach circumvents the issue of choosing one objective function and allows prioritization of the objectives (that is, design metrics) and constraints.

Theory

This section presents the multiobjective optimization and physical programming concepts used in this work.

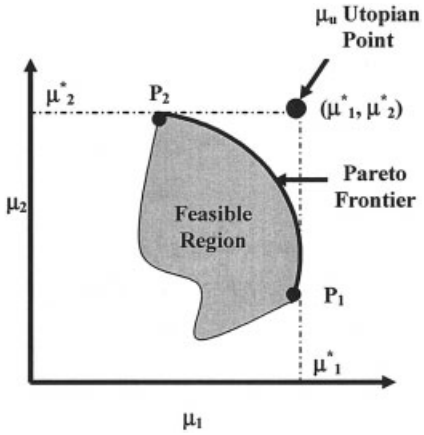

Figure 1. Pareto Frontier for a general bi-objective space.

Multiobjective optimization

Definitions

(1) *Multiobjective optimization*. A multiobjective optimization is a problem involving several competing objectives and constraints. The solution of this problem is considered the best solution that satisfies the conflicting objectives. Other commonly used terms in the literature for multiobjective optimization are multicriteria optimization, multidecision optimization, and vector optimization.

(2) *Pareto solution*. A Pareto solution is one where any improvement in one objective can take place only at the cost of another objective. A Pareto set is a set of Pareto-optimal solutions.

(3) *Design parameters*. A design parameter is a parameter over which the designer has direct control (such as gradient slope, feed load, and flow rate). Other terms used in the literature for design parameters include decision variables, design variables, or decision parameters.

(4) *Design metric*. A design metric refers to an objective measure of a design attribute. Other commonly used terms are objective functions, design criterion, figure-of-merit, goal, and performance metric. Design metrics include production rate, yield, and product pool concentration. In the current work, the variable $\mu(x)$ denotes the vector of design metrics and is related to the design parameters using simulations obtained from a general rate model of chromatography described elsewhere (Nagrath et al., 2004). In this paper's physical programming formulation, yield, and product pool concentration are included as soft design metrics.

(5) *Design constraint*. A design constraint indicates the lower or upper bounds in the design metrics or design parameters.

(6) *Anchor value*. The value obtained for a particular design metric if that design metric alone is optimized, given the bounds on the design parameters.

Pareto Concept. Figure 1 presents a schematic of a Pareto set for a bi-objective problem. If design metric μ_1 alone is optimized (maximized), then the optimal value is μ_1^* (shown as point P_1). Similarly, if design metric μ_2 alone is optimized then the optimal value is μ_2^* (shown as point P_2). Here μ_1^* and μ_2^* are the anchor values for design metrics μ_1 and μ_2, respectively. The ideal or utopian solution (μ_1^*, μ_2^*), obtained by the individual maximization of the objective functions, is generally not a feasible solution of the multiobjective optimization problem. As seen in Figure 1, the arc joining points P_1 and P_2 defining the boundary of the feasible space is the efficient Pareto frontier. That is, for every point on arc P_1–P_2, it is not possible to improve both objectives simultaneously. If one objective is improved, it must be at the expense of the other. Points on the arc are often referred to as *Pareto points* and are the candidates of choice in the process of multiobjective optimization. In engineering applications, the designer is often presented with several Pareto optimal points, representing alternative designs, from which one selects the value that offers the best trade-off among multiple objectives. In this work we use Pareto plots to qualitatively evaluate various optimization scenarios for linear gradient chromatography of protein mixtures.

Normal constraint method for generation of Pareto frontiers

Herein, the Pareto frontiers were generated using a novel normalized normal constraint (NNC) method developed by Ismail and Messac (2002). NNC possesses favorable properties compared with those of other methods (such as weighted sum) and redresses numerical scaling deficiencies of generic multiobjective methods. The development of Pareto frontiers provides a qualitative framework to assess the optimal solution possibilities and allows the designer to investigate the interplay between the design metrics.

Physical programming

Physical programming is a method that uses physically motivated information from the design engineer as inputs to formulate an optimization problem reflecting the designer's preferences. In the physical programming method, these preferences are directly expressed in the aggregate objective function and the steps involved in this approach are depicted in Figure 2.

Design Metrics. The design metrics are denoted by the μ_i variables, which are components of the vector $\boldsymbol{\mu} = (\mu_1, \ldots, \mu_m)$. Design metrics may be quantities that the designer wants to minimize; maximize; take on a certain value (goal); fall in a particular range; or be less than, greater than, or equal to particular values. The industrial manufacturer can define a preference with respect to each design metric by providing certain numerical values. The design metric then becomes part of an *aggregate objective function* (AOF) to be minimized or to be treated as an inequality or equality constraints on the aggregate objective function.

Objectives and Class Functions. In the physical programming method, objectives can be expressed with respect to each design metric using different Classes. Each Class consists of two cases, Hard and Soft, referring to the "sharpness" of the preference. The desired behavior of a generic design metric is described by one of eight sub-Classes: four Soft and four Hard, as shown in Table 2a. For each of these Classes, a Class function is formed that provides the means for a designer to express the spectrum of preferences for a given design metric. The Class functions provide information that is deliberately imprecise. By design, the utopian value of a Class function is

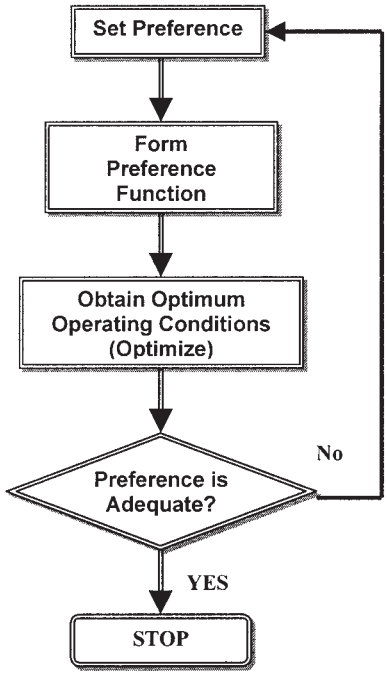

Figure 2. Physical programming approach for design and optimization.

zero. All Soft Class functions become constituent components of the aggregate objective function. Figure 3 qualitatively depicts different types of Soft Class functions. The value of the design metric under consideration, μ_i, is on the horizontal axis, and the function that will be minimized for that objective, $P_i(\mu_i)$, hereby called the Class function, is on the vertical axis. There are six ranges for each generic design metric for Classes 1S and 2S, 10 ranges for Class 3S, and 11 for Class 4S. To illustrate this, consider the case for Class 1S. The ranges are defined in order of decreasing preference as follows:

- *Highly Desirable* ($\mu_i \leq \nu_{i1}$): An acceptable range that is high desirable.
- *Desirable* ($\nu_{i1} \leq \mu_i \leq \nu_{i2}$): An acceptable range that is desirable.
- *Tolerable* ($\nu_{i2} \leq \mu_i \leq \nu_{i3}$): An acceptable, tolerable range.
- *Undesirable* ($\nu_{i3} \leq \mu_i \leq \nu_{i4}$): A range that, although acceptable, is undesirable.
- *Highly Undesirable* ($\nu_{i4} \leq \mu_i \leq \nu_{i5}$): A range that, although still acceptable, is highly undesirable.
- *Unacceptable* ($\mu_i \geq \nu_{i5}$): The range of values that the generic objective may not take.

The parameters ν_{i1} through ν_{i5} are *physically meaningful* constants that are specified by the designer to quantify the preferences associated with the *i*th design metric. The corresponding Class functions map design metrics into nondimensional, strictly positive real numbers. This mapping, in effect, transforms design metrics with disparate units and *physical* meaning onto a dimensionless scale through a unimodal function. Figure 3 illustrates the mathematical nature of the Class functions and shows how they allow designers to express the ranges of preferences for different classes. Preferences regarding each design metric are treated independently, allowing the inherent multiobjective nature of the problem to be preserved. The value of the Class function for each design metric governs the optimization path in objective space.

Physical Programming Formulation. Figure 4 illustrates various mappings that take place between design parameters and the aggregate objective function in physical programming. The first part of the mapping is between design parameters (also defined as the decision variables) and design metrics. The mapping between design parameters (such as feed load, flow rate, salt gradient) and design metrics is carried out using appropriate chromatographic models described elsewhere (Nagrath et al., 2004). The "goodness" of a design metric, or $P_i(\mu_i)$, is dictated by the preference function assigned by the designer. $P_i(\mu_i)$ depends on the value of a design metric (μ_i), on the class type (Table 2a) assigned to the design metric, and on the range of preference values associated with the design metric (such as ν_{i1} to ν_{i5}). The class functions are obtained using the designer preferences on the objective function. The next step involves the formation of an aggregate objective

Table 2a. Characterization of Classes

Soft		Hard	
Class 1S	Smaller-is-better: minimization	Class 1H	Must be smaller: $\mu_i \leq \mu_{i,\max}$
Class 2S	Larger-is-better: maximization	Class 2H	Must be larger: $\mu_i \geq \mu_{i,\min}$
Class 3S	Value-is-better	Class 3H	Must be equal: $\mu_i = \mu_{i,\min}$
Class 4S	Range-is-better	Class 4H	Within range: $\mu_{i,\min} \leq \mu_i \leq \mu_{i,\max}$

Table 2b. Characterization of Chromatographic Design Metrics into Different Classes

Design Metric	Class Functions	Desirability
Production rate	Class 2S	Larger is better: Maximization
Production rate times yield	Class 2S	Larger is better: Maximization
Product pool concentration	Class 2S	Larger is better: Maximization
Solubility constraint	Class 1H	Must be less than
Yield	Class 2S or Class 2H	Maximization or must be greater than
Purity	Class 2H	Larger is better: Maximization

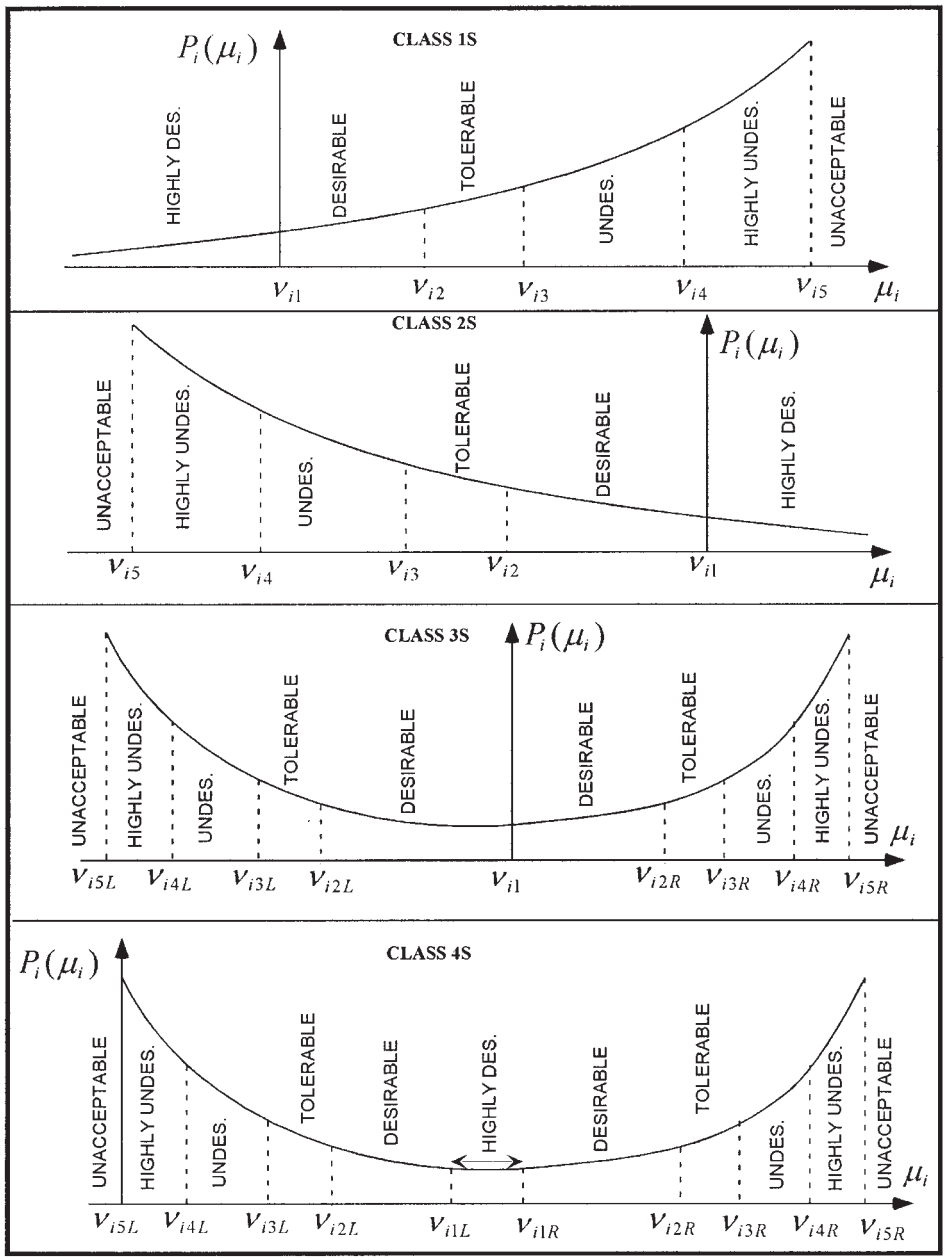

Figure 3. Soft class function ranges for the *i*th generic design metric.

function, which is the sum of all the class functions. After the completion of the mapping, the aggregate objective function is then minimized using nonlinear programming. The physical programming problem is represented mathematically as

$$J = \min_x P[\mu(x)] = \left\{ \frac{1}{n_{sc}} \sum_{i=1}^{n_{sc}} P_i[\mu_i(x)] \right\}$$

subject to

$$\begin{aligned}
&\mu_i \le v_{i5} && \text{(for class 1S design metrics)}\\
&v_{i5} \le \mu_i && \text{(for class 2S design metrics)}\\
&v_{i5L} \le \mu_i \le v_{i5R} && \text{(for class 3S design metrics)}\\
&v_{i5L} \le \mu_i \le v_{i5R} && \text{(for class 4S design metrics)}\\
&\mu_i \le v_{iM} && \text{(for class 1H design metrics)}\\
&\mu_i \le v_{im} && \text{(for class 2H design metrics)}\\
&v_i(x) = \mu_{iv} && \text{(for class 3H design metrics)}\\
&v_{im} \le \mu_i(x) \le v_{iM} && \text{(for class 4H design metrics)}\\
&x_{jm} \le x_j \le x_{jM} && \text{(for design var. constraints)}
\end{aligned}$$

where v_{im}, v_{iM}, x_{jm}, and x_{jM} represent maximum and minimum values, and the μ_{iv} defines the equality constraints; the range

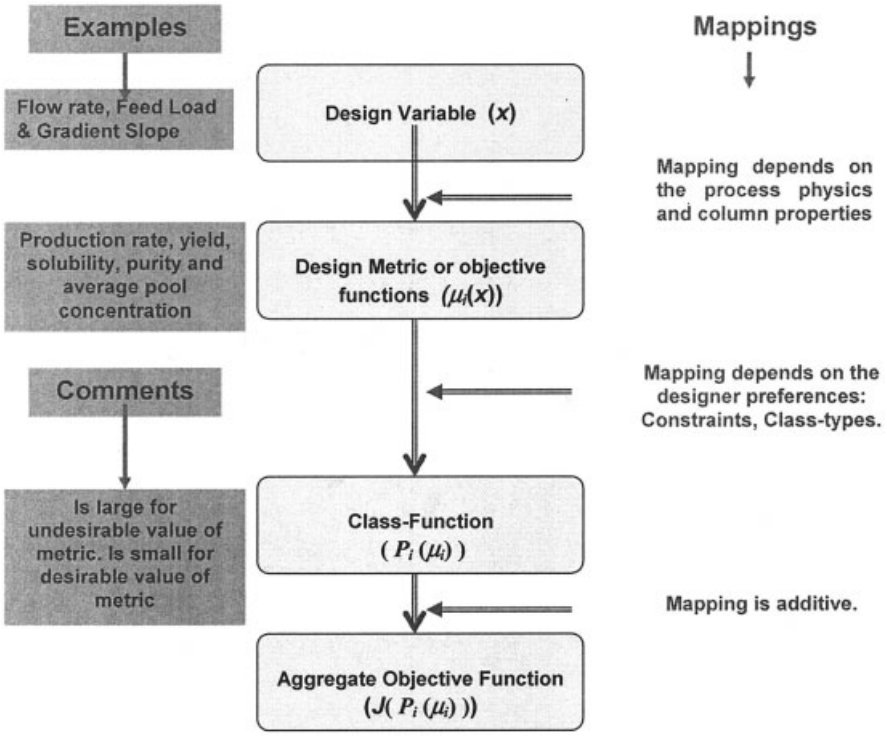

Figure 4. Physical programming mappings.

limits are provided by the designer; the number of soft design metrics that the problem constitutes is represented by n_{sc}.

The previous discussion provides a cursory presentation of physical programming, which is sufficient to understand how it is applied. For more details the interested reader is invited to examine the following references: Messac (1996, 2000), Messac and Chen (2000), and Messac et al. (1996, 2000). Not only is physical programming a powerful method for multiobjective optimization, but it can be readily implemented in MATLAB.

Physical Programming Visualization

As discussed previously, the physical programming paradigm calls for the designation of ranges of different degrees of desirability for each design metric. The versatility of this approach also stems from the fact that it aids in simultaneously visualizing a large number of design metrics. The numerical values of the objective functions are mapped to account for the a priori–expressed preference of the designer and a bar graph is used to represent the instantaneous value of each design metric (Figure 5). This facilitates the dynamic assessment of the effect of the preference specifications on the objectives as well as the complex interplay of these objectives. Figure 5 shows the visualization process for a representative case of the gradient separation of a binary mixture (α-chymotrypsinogen A and ribonuclease A). In the color-coded background on the figure, a bar graph (on the right) is used to represent the instantaneous value of each design metric in real time. The figure is subdivided into nine horizontal sections that correspond to regions of differing degree of desirability. Each section is then color coded according to the desirability level and is labeled appropriately. For the case presented here, there are three design metrics (production rate, yield, and solubility constraint). For clarity, visualization is shown for production rate and yield. As seen in the figure, at the 50th optimization run the production rate is in the highly undesirable region and yield is in the highly desirable region. However, at the end of the 100th iteration, the values of both production rate and yield are between the desirable and tolerable regions. [Note: because a hybrid model is used for these simulations, the computation time is minimal (Nagrath et al., 2004).] Clearly, this approach permits the visualization of the complex interplay between production rate and yield. Although results shown here include only two design metrics, the visualization of design metrics in this form can be easily carried out for any number of design metrics.

Results and Discussion

In chromatographic separations, the desired objectives and/or constraints can be described according to a hierarchy and assigned different levels of priority. Thus, the optimization problem can be posed as a wide-range multiobjective optimization, which leads to the development of a systematic method for describing the design objective preferences and constraint handling. For example, in protein chromatography high recovery yields are often required, and thus yield should be included either as a constraint or as a component of the aggregate objective function. Further, it is often desirable to minimize dilution during the chromatographic process and to have a high product pool concentration (subject to solubility constraints). Consequently, we investigate the effect of the product pool concentration as one of the additional design metrics.

In the current work, all of the optimization results use hybrid models described elsewhere (Nagrath et al., 2004) for model development. Briefly, transport and isotherm parameters are

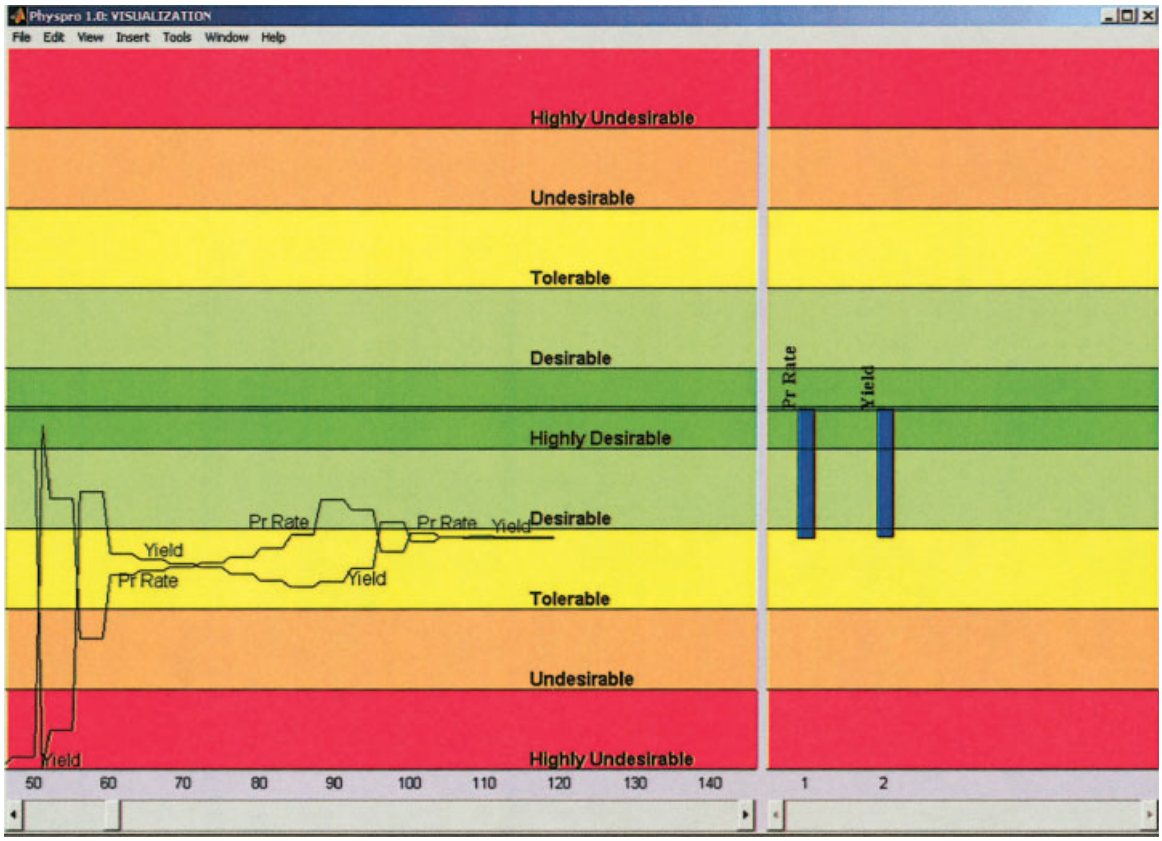

Figure 5. Physical programming visualization window.

The top four sections permit the visualization of design metrics that are minimized, whereas the bottom four sections are used for visualizing design metrics that are maximized. The middle section is common to both maximization and minimization of design metrics.

experimentally determined using techniques previously developed in our group (Gadam et al., 1992; Natarajan et al., 2000b). The resulting parameters are then used in the physical model (the general rate model of chromatography in concert with the nonequilibrium steric mass action adsorption isotherm) for parametric simulations to generate data for *n*-dimensional response surfaces that relate the production rate, yield, purity, and product pool concentration to the other parameters of the system (such as feed load, flow rate, salt gradient). These simulations are performed on a high-speed parallel computing cluster at Rensselaer. The resulting data sets of design metrics for various design parameters were then used to develop an empirical model for each feed component in this system. A multilayer artificial neural network (ANN) model is then used to represent these response surfaces. The final configuration of the resulting ANN-based hybrid models is: $16 \times 11 \times 8 \times 4$ for the first component; $14 \times 12 \times 9 \times 4$ for the second component; and $16 \times 11 \times 8 \times 4$ for the third component. ANN topology optimization and learning procedure used for the current study is explained elsewhere (Nagrath et al., 2004). This ANN model is used herein for multiobjective optimization.

As discussed previously, physical programming can be formulated in any multiobjective optimization framework (either a priori, a posteriori, or interactive methods). Because we first use Pareto frontiers in a qualitative analysis and then use them for progressive articulation of preferences, our approach falls under the category of interactive methods. As described in the theory section, physical programming requires characterization of design metrics into different classes. Table 2a presents the general classes possible for any optimization problem. The characterization of various design metrics relevant to chromatographic processes and used in the current work is presented in Table 2b.

First, we investigate the gradient separation of a binary protein system (α-chymotrypsinogen A and ribonuclease A). We then examine a tertiary mixture (α-chymotrypsinogen A, ribonuclease A, and a later eluting artificial component) for both bi-objective and tri-objective cases at different levels of purity. In all of the cases examined herein, the solubility constraint was satisfied using a hard constraint (Class 1H) on the maximum solute concentration (set to be <5 mM).

Binary systems

This section presents the optimization results for the linear gradient separation of a binary protein mixture (α-chymotrypsinogen A and ribonuclease A). Figure 6 shows the Pareto frontiers of both the early and later eluting components. As seen in the figure, the trade-off between production rate (denoted as μ_1) and yield (denoted as μ_2) becomes increasingly pronounced at higher production rates for both components. It can also be seen that the Pareto frontiers have a sharp decrease for the later eluting component. This exemplifies that the

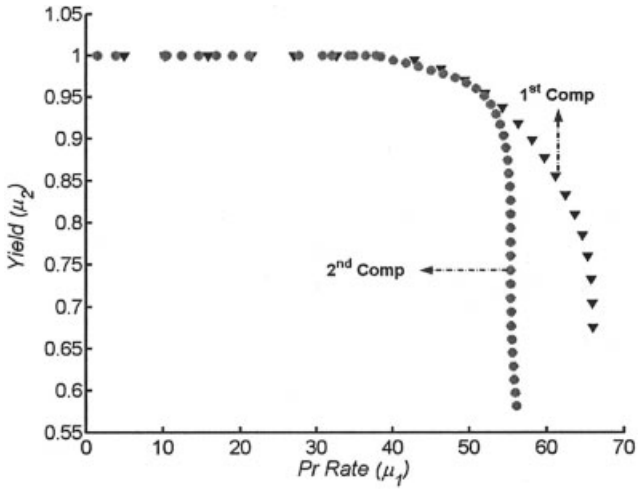

Figure 6. Pareto frontiers for two model proteins, α-chymotrypsinogen A and ribonuclease A on 90 μm FF Sepharose stationary phase.

Column conditions are: diameter 1.6 cm; length 10.5 cm. Feed conditions are: ribonuclease A and α-chymotrypsinogen A at 0.7 mM each. The 1st component is the early eluting ribonuclease A and the 2nd component is the later eluting α-chymotrypsinogen A. The triangles and the circles are the Pareto solutions for optimization of the early and later eluting components, respectively.

optimization of production rate is more difficult for a later eluting component compared to that of an early eluting component. This is because at higher production rates for the later eluting component, only a small amount of change in production rate can be attained for a large change in yield. Furthermore, processes operated at a higher production rate, where the later eluting compound is the desired product, may not be robust because small process variability may lead to a large decrease in the yield.

Tertiary systems

To examine a more complex separation, a ternary mixture consisting of α-chymotrypsinogen A, ribonuclease A, and a later eluting artificial component (Nagrath et al., 2004) was investigated. We first examine the Pareto frontiers of all three components at the 95% purity level to obtain qualitative information, and then use physical programming for their optimization. The Pareto frontiers can be used to infer the design objective preference range and qualitative information about the design metrics, which are then used in physical programming to specify the preferences for the design metrics. The effect of purity as an independent design parameter is further investigated by observing its effect on the later eluting component. Finally, we investigate the effect of the product pool concentration as one of the additional objectives for the third component. This is carried out first for a bi-objective scenario and then for a tri-objective scenario.

Tertiary mixture for bi-objective system at a fixed purity

Figure 7a presents the Pareto frontiers of a tertiary mixture (ribonuclease A, α-chymotrypsinogen A, and a later eluting artificial component) at 95% purity. The first component is the early eluting ribonuclease A, the second component is α-chymotrypsinogen A, and the third component is the later eluting artificial component. It is important to note that the Pareto frontier of the second component is below the frontiers of the other components because it experiences overlap from both the first and third components. It is also worth noting that the "anchor values" of the production rate for the first and second components occur at significantly higher yields than those for the third component. Again, the anchor value is defined as the value obtained for a particular design metric if that design metric alone is optimized, given the bounds on the design parameters (such as flow rate and gradient slope).

To explore these scenarios in more detail, it is instructive to examine the outlet concentration profiles from the simulations. Figures 7b–d show the outlet concentration profiles for the scenarios in which the component of interest is the first, second, and third, respectively. In each of the panels b–d of Figure 7, the outlet concentration profiles are depicted for two operating conditions, one in which the desired component has a production rate at a reasonable yield (Case 1) and the other in which the desired component has a high production rate at low yield (Case 2). The operating conditions for these six cases (two for each component) are indicated in Figure 7a and presented in Table 3. Cases 11P and 12P are for scenarios where the desired component is the first component. In particular, Case 11P is at a relatively high yield and low production rate; and Case 12P is for a high production rate and low yield. From Figure 7b, it can be seen that at the high feed loading (12P), the front of the first component becomes sharper and its maximum concentration increases as a result of sample displacement. However, there is a concomitant increase in overlap between the first and second components, which leads to a decrease in yield.

In Cases 21P (relatively high yield) and 22P (high production rate), the desired component is the second component. As seen in Table 3, the optimal values of the design metrics (production rate and yield) and parameters (flow rate, gradient slope, and feed load) are low for this case when compared with the optimization results for the first and third components (at a constant purity constraint of 95%). Again, this is because the overlap of the second component with the other two solutes and the low separation factor between individual components limits the column loadings to moderate values. In addition, as seen in Figure 7c, the maximum concentrations of solutes are lower than those for the cases shown in Figures 7b and d.

When the third component is desired, for cases 31P (high yield) and 32P (low production rate), a sharp decrease in the yield is observed at higher production rates (Figure 7a). As seen in the outlet concentration profiles in Figure 7d, the tailing of the second component leads to a reduced production rate of the third component. The optimal design parameters (flow rate, gradient slope, and feed load) when the third component is desired at high yield (31P) are lower than those obtained when the first component is desired (11P). This is because the separation factor between the second and third components is lower than that between the first and second components, thus restricting the column loading to moderate values. Further, sample displacement effects increase the yield of component 1, but not that of component 3.

To investigate the interplay between various design metrics in this system we will focus the rest of the discussion on the

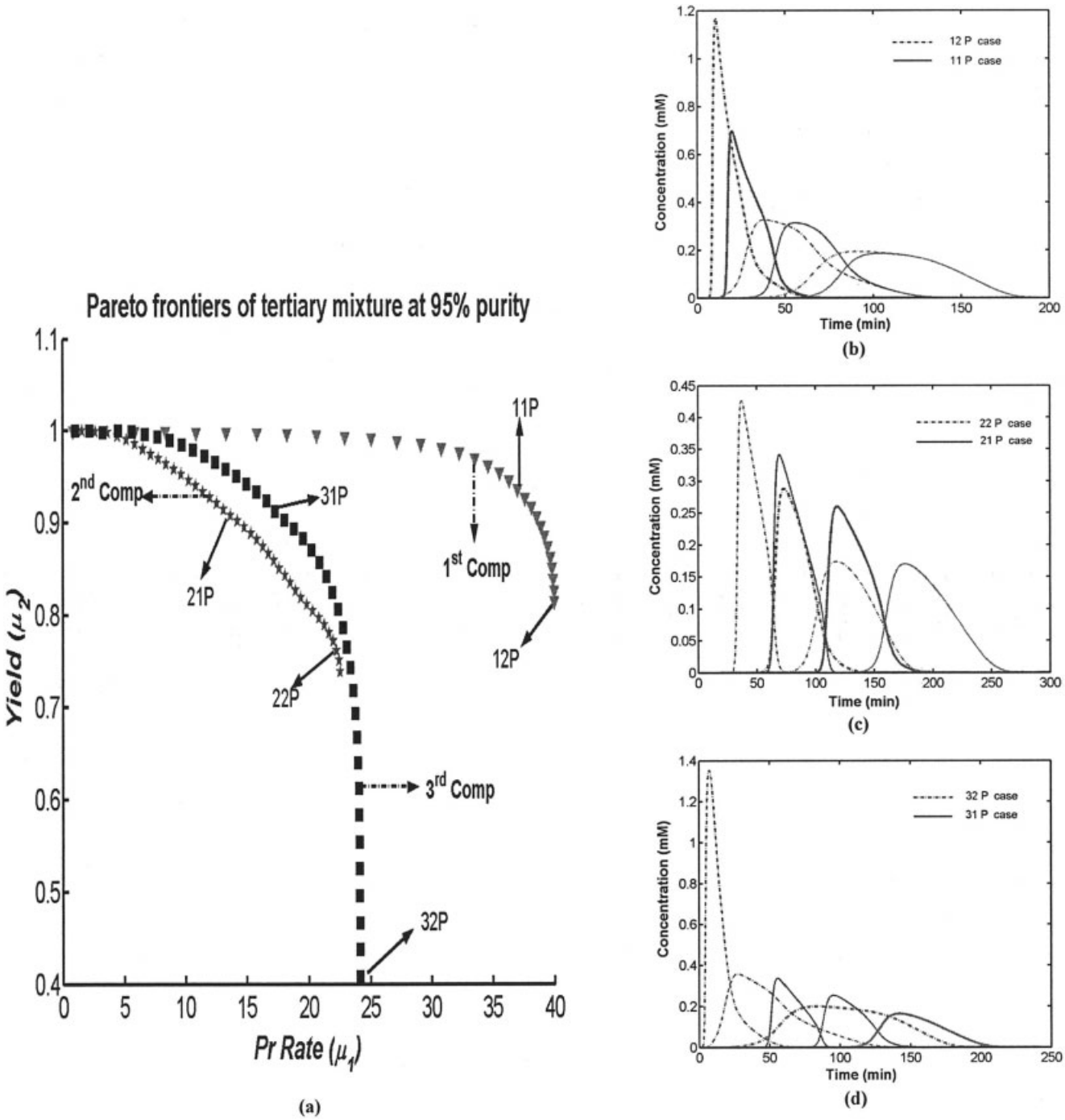

Figure 7. Pareto frontiers and outlet concentration profiles for a tertiary mixture (α-chymotrypsinogen A, ribonuclease A, and artificial component) on a 90 μm FF Sepharose stationary phase.

The 1st component is the early eluting ribonuclease A, the 2nd component is the middle eluting α-chymotrypsinogen A, and the 3rd component is the later eluting artificial component. The triangles, stars, and squares are the Pareto solutions for the optimization of the first, second, and later eluting components, respectively. Outlet concentration profiles for the tertiary mixture for the six cases indicated in (a) are shown in (b), (c), and (d) when the component of interest is the first, second, and the third component, respectively. Column conditions are: diameter 1.6 cm; length 10.5 cm. Feed conditions are: ribonuclease A, α-chymotrypsinogen A, and the artificial component at 0.5 mM each. The average separation factor between ribonuclease A and α-chymotrypsinogen A is 1.55, and is 1.35 between α-chymotrypsinogen A and an artificial eluting component (Nagrath et al., 2004).

optimization of the third component. The reason for this is that there is a larger trade-off region for this component (Figure 7a) and the sharp Pareto frontier makes production rate optimization difficult compared to that of yield.

The effect of purity constraints

In this section we investigate the effect of purity as an independent parameter on the optimal values of design metrics and design parameters of the later eluting artificial component.

Table 3. Optimal Design Parameters for Various Cases Shown in Figure 7a

Desired Component	Case	Optimal Production Rate (mmol min^{-1} mL^{-1})	Optimal Yield (%)	Optimal Flow Rate Fl* (mL/min)	Optimal Gradient Slope GS* (mM/DCV)	Optimal Gradient Slope GS* (mM/min)	Optimal Feed Load TF* (DCV)
First	11P	36.92	93.68	4.59	1	0.7	13.37
	12P	39.88	81.52	4.59	1	0.7	16.62
Second	21P	13.68	90.79	3.21	1	0.49	7.26
	22P	22.26	76.04	4.59	1	0.7	9.46
Third	31P	17.27	91.24	4.03	1	0.62	7.3
	32P	24.12	43.84	4.59	1	0.7	19.98

Note: DCV denotes the dimensionless column volume.

The Pareto frontiers at three different purities—91, 95, and 99% for a later eluting component—are shown in Figure 8a. As seen in the figure, the "anchor value" of the production rate for the later eluting component deceases with increasing purity. In addition, there is an overall increase in the trade-off region (Pareto optimal) of design metrics at the higher-purity constraints. Because the Pareto frontier at 99% purity is "below" the frontiers of the other components, increasing the purity constraint clearly results in a decrease of both the optimal yield and production rate. Interestingly, the 99% purity Pareto frontier has a noticeable difference when compared with Pareto curves at other purities: there is a continuous sharp decrease in yield from the low to high production rate regions. In contrast, in the other Pareto frontiers yield generally decreases at a

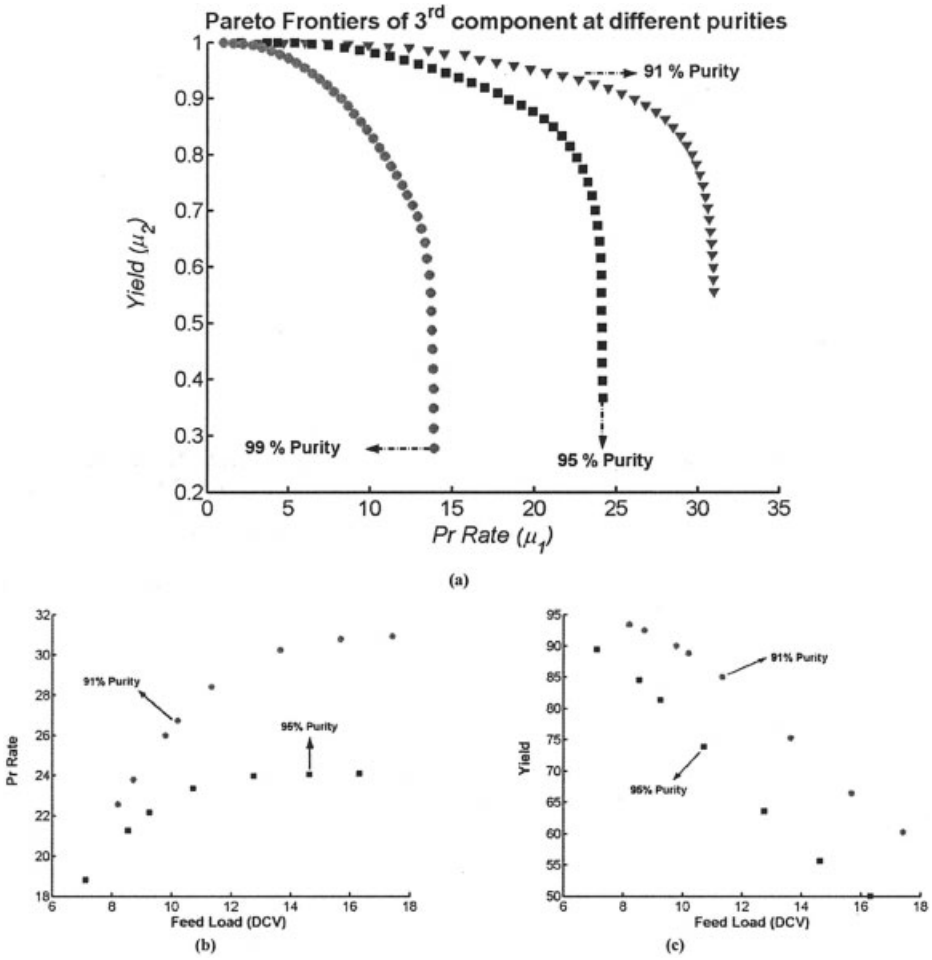

Figure 8. (a) Pareto frontier of the later eluting component at three different purities in a tertiary mixture (α-chymotrypsinogen A, ribonuclease A, and the later eluting artificial component) on a 90 μm FF Sepharose stationary phase.

The triangles, squares, and circles are the Pareto solutions for optimization at 91, 95, and 99% purity constraints, respectively. Variations of the design metrics production rate and yield with feed load at 91 and 95% purity constraint for the later eluting component are shown in (b) and (c), respectively. Column conditions are: diameter 1.6 cm; length 10.5 cm. Feed conditions are: ribonuclease A, α-chymotrypsinogen A, and the artificial component at 0.5 mM each.

Table 4. Physical Programming Optimization Results for the Later Eluting Artificial Component in a Tertiary Mixture for a Bi-Objective System (Production Rate and Yield) at 99, 95, and 91% Purity Constraints

RN\CN	1	2	3	4	5	6	7	8	9	10	11	12	13	14	15
	Preferences—Pr Rate					Opt. Value	Preferences—Yield					Opt Value	Opt. Design Parameters		
	HUD	UD	T	D	HD	PR*	HUD	UD	T	D	HD	Yield*	Fl*	GS*	TF*
99% Purity Constraint															
1	4	7●	10	13	16	8.44	80	84.5	89●	93.5	98	89.28	2.8	1	5.23
2	6	9●	12	15	18	9.28	80	84.5	●89	93.5	98	86.4	3.13	1	5.33
3	9●	11	13	14	15	9.88	80	●84.5	89	93.5	98	84.1	3.38	1	5.41
4	9	●11	13	14	15	10.84	75	79.5●	84	88.5	93	80.03	3.78	1	5.57
5	9	11●	13	14	15	12.43	65	68	71●	74	77	71.88	4.52	1	5.96
6	11	12.5	●13.5	14.5	16	13.46	50	54	58	●62	64	61.71	4.59	1	7.41
7	4	6●	8	10	12	6.72	89	91.5	●94	96.5	99	93.9	2.18	1	5.1
8	4	●6	8	10	12	5.98	94	95●	96	97	99.5	95.48	1.92	1	5.05
9	2	3	4	5●	6	5.04	94	95	96	97●	99.5	97.11	1.6	1	5.03
10	2	3●	4	5	6	3.45	97	98.5	99●	99.5	99.9	99.01	1.24	1	4.35
95% Purity Constraint															
1	5	10	15●	20	25	16.89	80	84.5	89	●93.5	98	92.05	4.06	1	7.02
2	13	16	●19	22	25	18.82	80	84.5	89●	93.5	98	89.49	4.59	1	7.11
3	19	●22	25	28	31	21.28	80	84.5●	89	93.5	98	84.58	4.59	1	8.53
4	19	22	●25	28	31	23.38	65	68	71	●74	77	73.94	4.59	1	10.71
5	19	22	●25	28	31	23.98	50	54	58	62●	66	63.59	4.59	1	12.75
6	22	●25	28	31	34	24.07	42	46	50	54●	58	55.67	4.59	1	14.63
7	23	●25	27	29	31	24.1	38	42	46	50●	54	50.05	4.59	1	16.32
8	5	10	15●	20	25	15.56	84	88	92	●94	99	93.57	3.78	1	6.83
9	4	8	10	●12	14	11.72	90	93	96	●98	99	97.14	2.94	1	6.38
10	4	5	6	7	●8	7.78	95	97	98	99●	99.9	99.34	1.98	1	6.14
91% Purity Constraint															
1	15	19	23●	27	31	23.79	84.5	88	91.5	●94	98	92.49	4.59	1	8.72
2	20	25●	30	35	40	26.00	84.5	88	●91.5	94	98	90.04	4.59	1	9.79
3	20	25●	30	35	40	26.73	80	84.5	●89	93.5	98	88.92	4.59	1	10.20
4	20	25●	30	35	40	28.41	75	79.5	84●	88.5	93	85.10	4.59	1	11.34
5	20	25	30●	35	40	30.26	65	68	71	74●	77	75.32	4.59	1	13.64
6	20	25	30●	35	40	30.78	50	54	58	62	66●	66.51	4.59	1	15.69
7	30●	35	40	45	50	30.94	50	54	58	●62	66	60.27	4.59	1	17.41
8	15	19	●23	27	31	22.57	88	91	●94	97	99.5	93.44	4.59	1	8.2
9	15	19	●23	27	31	20.06	92	94	●96	98	99	95.08	4.1	1	8.01
10	10	12	14●	16	18	14.71	96	97	98●	99	99.9	98.25	3.29	1	7.05
11	8	9	10	11●	12	11.81	97	97.5	98.5	99●	99.9	99.17	2.63	1	7.02

Note: For a 99% purity constraint system: In Cases 2–6 higher production rate is desired, whereas in Cases 7–10 higher yield is desired. For a 95% purity constraint system: In Cases 2–7 higher production rate is desired, whereas in Cases 8–10 higher yield is desired. For a 91% purity constraint system: In Cases 2–7 higher production rate is desired, whereas in Cases 8–10 higher yield is desired. The upper bound specified on flow rate, gradient slope, and feed load in the physical programming of a binary mixture (α-chymotrypsinogen A and ribonuclease A) is 4.59 (mL/min), 22 (mM/DCV), and 22 (DCV), respectively. The lower bound specified on flow rate, gradient slope, and feed load is 0.1 (mL/min), 1 (mM/DCV), and 1 (DCV), respectively. DCV denotes the dimensionless column volume.

relatively slow rate in the low to medium production rate regions and exhibits a sharp decrease only under high production rate conditions.

The physical programming optimization results for various preferences and preferentially desired design metrics for the 99% purity scenario are presented in the top section of Table 4. The preference ranges for the physical programming optimization were selected as 2–18 (mmol min^{-1} mL^{-1}) for the production rate and 50–99.5% for the yield. The optimal values of design metrics obtained for the base case (Case 1) are 8.44 (mmol min^{-1} mL^{-1}) and 89.28% for the production rate and yield, respectively. In Cases 2–6 higher production rate is desired, whereas in Cases 7–10 higher yield is desired. To increase the optimal value of production rate, the preference values for the production rate are increased in Cases 2–3, whereas yield preferences are maintained at a constant value. This is achieved by increasing the flow rate and feed load. To further increase the production rate, the preferences for the yield are decreased in Cases 4–5 and those of the production rate are maintained at a constant value. To achieve a higher value of the production rate, it is not sufficient to just increase the preferences of production rate; it is also necessary to decrease the preferences for the yield. Accordingly, a simultaneous increase in the production rate preference and decrease in the yield preference is prescribed in Case 6, which results in a significant increase in the production rate at the cost of a decreased yield. As is seen in Cases 7–10, a high value of yield requires a decrease in the preferences for production rate. To achieve these higher yield values, both feed load and flow rate must be decreased.

In fact, the results in Table 4 for a 99% purity constraint system indicate that when the later eluting solute is the desired component in a tertiary mixture, the optimal values of design parameters were the following: low to medium flow rate; low gradient slope; and variable feed load to attain a desired production rate and yield. Here, reduced flow rate is required because the high-purity constraint does not allow much mixing between the zones, and mass transport limitations can come into play.

The middle section of Table 4 presents the physical pro-

gramming optimization results for a 95% purity constraint. The preference ranges in the physical programming optimization for the 95% purity scenario were selected as 4–31 (mmol min^{-1} mL^{-1}) for the production rate and 38–99.9% for the yield. In Cases 2–8 higher production rate is desired, whereas in Cases 9–11 higher yield is desired. The optimal values of design metrics obtained for the base case (Case 1) are 16.89 (mmol min^{-1} mL^{-1}) and 92.05% for the production rate and yield, respectively. An increase in the optimal value of production rate is achieved in Cases 2–3, by increasing the specified preferences of the production rate itself, while keeping the yield preferences the same. As seen in the table, there is a steady increase in production rate with a corresponding decrease in the yield. To further increase the production rate, the preferences for the yield are decreased in Cases 4–7 and those of the production rate are maintained at constant (and unrealistic) values. As seen in the table, because the production rate preferences are for the most part beyond the maximal Pareto optimal value, there is minimal increase in the production rate with concomitant significant decreases in the yield. Clearly, this is not acceptable.

In Cases 8–10, higher optimal values of yield are achieved by first increasing the preferences for yield (Case 8), and later (Cases 9–10) by simultaneously increasing the yield preferences and decreasing the preferences for the production rate. Interestingly, if the desired yield is below 90% then the optimal flow rate for this case is the maximal attainable value of 4.59 mL/min. Thus, in contrast to the results with 99% purity where the maximal flow rate was possible only for low yields (such as 61.7%), for 95% purity the maximal flow rate can be used for any case where the yield is $<90\%$.

The bottom section of Table 4 presents the physical programming optimization results for a 91% purity constraint. The preference ranges in the physical programming optimization for the 91% purity scenario were 8–50 (mmol min^{-1} mL^{-1}) for the production rate and 70–99% for the yield. In Cases 2–7 higher production rate is desired, whereas in Cases 8–11 higher yield is desired. In Cases 2–7, the maximal flow rate value is obtained. Cases 6 and 7 show that because the production rate preferences are for the most part beyond the maximal Pareto optimal value, there is minimal increase in the production rate with concomitant significant decreases in the yield. At this level of purity constraint, the maximal flow rate is obtained for all cases except for those of high yields ($>94\%$).

As was seen in the middle and the bottom sections of Table 4, to attain a higher yield, the flow rate was decreased from its maximal value. However, to attain higher production rates, the flow rate was maintained at its maximal value and feed load was the only design parameter varied. Figures 8b and c examine the relative effect of the feed load on the production rate and yield at two different purities (91 and 95%). As shown in Figures 8b and c, the effect of the optimal feed load on the yield is more pronounced than the effect on the production rate. At higher feed loads the increase of the production rate is low and the system exhibits saturation behavior arising from specified bounds on the design parameters. Further, it can be seen from the figure that the effect of feed load on the production rate is more pronounced at the 91% purity constraint.

At any feed load, as the gradient slope becomes higher, there is an increased mixed zone between closely retained components that decreases both the yield and purity of the desired component. It turns out that most of the optimal results presented in Table 4 for both 91 and 95% purity constraints correspond to relatively high feed loads. Under these conditions, sample displacement effects can become pronounced, resulting in significant narrowing of the bands. Under these conditions, any increase in the gradient slope can result in significant losses of material resulting from overlap of the narrow zones. Because all of the results in Table 4 for a later eluting component correspond to a relatively difficult separation at high feed loads, the physical programming optimization resulted in the lowest gradient slope for all of the scenarios. The program also resulted in the highest flow rate in most cases when low-purity constraint of 91 and 95% constraint was maintained. This is because the higher production rate attained at higher flow rates overshadowed any adverse transport effects at low-purity constraints. Under low to moderate feed load conditions, the production rate increases when loading is increased. However, under the higher feed load conditions, the production rate decreases because the narrowing of the bands overshadows the sharpening of the tails in these induced sample displacement profiles (Gallant et al., 1996). Accordingly, there are specific feed load conditions that will satisfy the various physical programming preference states.

Tertiary mixture with tri-objective system

Although dilution is a significant issue in batch chromatographic processes, product pool concentration has never been explicitly studied for the optimization of chromatographic processes. Accordingly, this section studies a coupling of a new objective function, product pool concentration, to the bi-objective systems studied in the previous section. First, we will study the effect of production pool concentration on the other design metrics (production rate and yield) using Pareto frontiers in a bi-objective scenario. We will then investigate the Pareto optimal surfaces and physical programming optimal results for the tri-objective scenario. The mapping between design parameters (feed load, flow rate, salt gradient) and design metrics (production rate, yield, product pool concentration, and maximum solute concentration) is carried out using the hybrid model strategy described elsewhere (Nagrath et al., 2004).

Before examining the tri-objective system, it is instructive to separately examine the interplay between the product pool concentration and the production rate and yield as presented in Figures 9a and b, respectively. As seen in Figure 9a, as the production pool concentration increases, there is a concomitant continual decrease in the production rate. For Figure 9b, as the product pool concentration increases there is a minimal change in the yield, until the Pareto frontier exhibits a sharp decrease. The Pareto frontiers at higher purity constraints are below the frontiers at lower purity constraints for both cases in Figures 9a and b. For the yield–product pool concentration bi-objective system (Figure 9b), increasing the purity reduces the product pool concentration anchor values. The reason for this is that an increase in the purity constraint produces a decrease in the optimum feed load, which in turn decreases the optimal product pool concentration.

Figures 9c and d present the Pareto surfaces of the later eluting component for a tri-objective system in a tertiary mixture at purities of both 95 and 99%. As seen in Figure 9c, as the product pool concentration increases, the trade-off region of

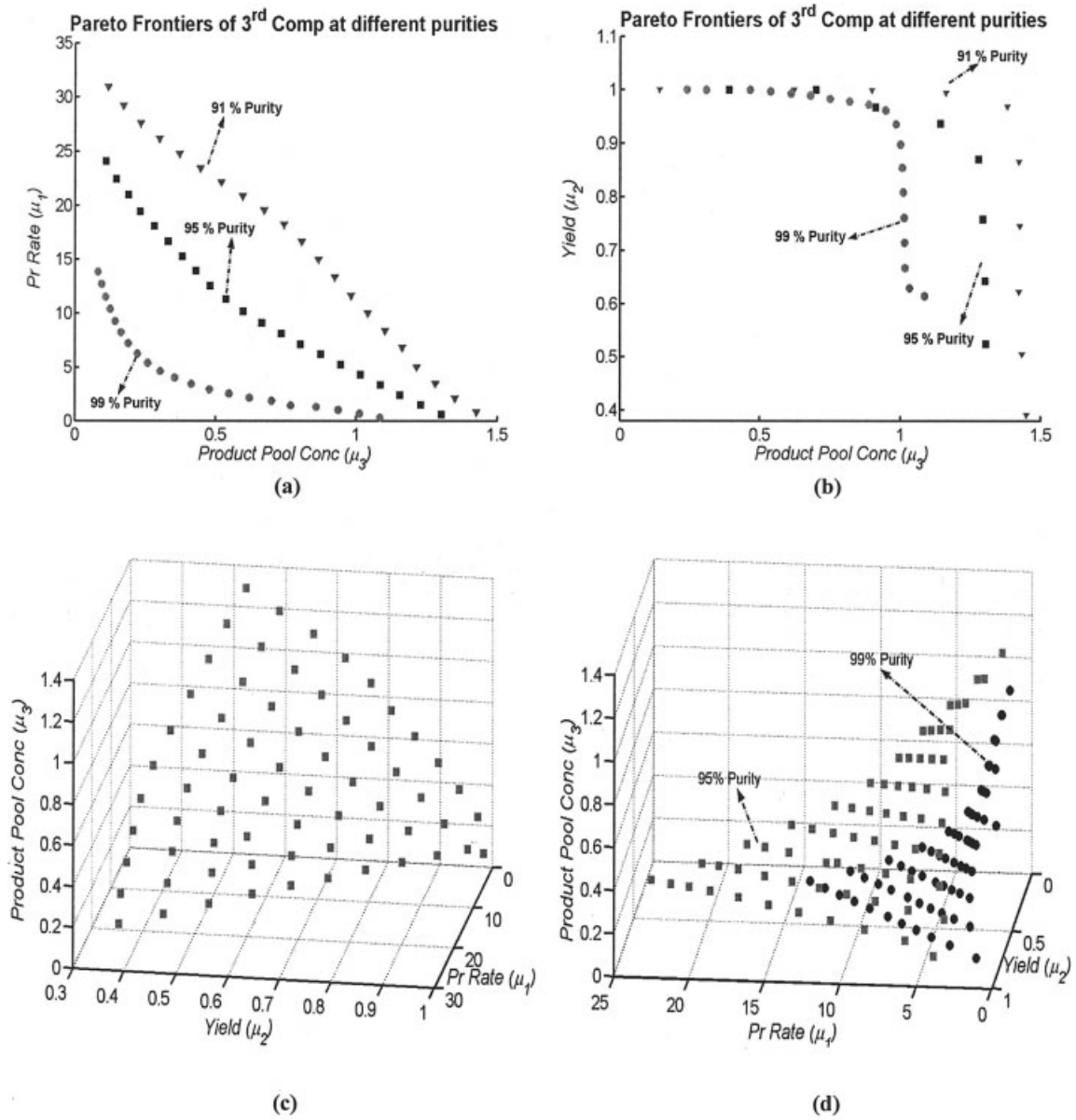

Figure 9. Pareto frontiers of the later eluting component at different purities in a tertiary mixture (α-chymotrypsinogen A, ribonuclease A, and artificial component) on a 90 μm FF Sepharose stationary phase for bi-objective and tri-objective systems.

(a) Production rate–product pool concentration bi-objective system. (b) Yield–product pool concentration bi-objective system. In (a) and (b), the triangles, squares, and circles are the Pareto solutions for optimization at 91, 95, and 99% purity constraints, respectively. Pareto surfaces of the later eluting component for a tri-objective (production rate, yield, and product pool concentration) setting, at two different purities in a tertiary mixture (α-chymotrypsinogen A, ribonuclease A, and the later eluting artificial component) are shown in (c) and (d). (c) Pareto surface at a 95% purity constraint; (d) comparison of Pareto surfaces at 95 and 99% purity constraints.

the Pareto surface between the production rate and the yield decreases for the 95% purity result. Figure 9d presents a comparison of the Pareto Frontiers at purities of 95 and 99%. Although both surfaces exhibit a sharp increase of product pool concentration with decreasing yield, the surface for 99% purity is shifted toward lower production rates. Also, the product pool concentration approaches its anchor value more sharply for the 99% purity constraint compared to that for the 95% constraint.

Table 5 presents the physical programming results for purity constraints of both 99 and 95%. The preference ranges in the physical programming optimization for the 99% purity scenario were 4–18 (mmol min^{-1} mL^{-1}) for the production rate, 50–98% for the yield, and 0.05–1.1 (mM) for the product pool concentration. The optimal values of design metrics obtained for the base case (Case 1) were 4.24 (mmol min^{-1} mL^{-1}), 85.09%, and 0.2 (mM) for the production rate, yield, and product pool concentration, respectively. Interestingly, the optimal feed load for all of these cases was relatively low because of the product pool concentration design metric.

To increase the optimal value of production rate, the preference values for the production rate are increased, whereas yield and product pool concentration preferences are decreased

Table 5. Physical Programming Optimization Results for a Later Eluting Component in a Tertiary Mixture for a Tri-Objective System (Production Rate, Yield, and Product Pool Concentration) at 99% and 95% Purity Constraints

RN\CN	1	2	3	4	5	6	7	8	9	10	11	12	13	14	15	16	17	18	19	20	21
	Preferences—Pr Rate					Opt. Value	Preferences—Yield					Opt. Value	Preferences—Product Pool Conc. (PPC)					Opt. Value	Opt. Design Parameters		
	HUD	UD	T	D	HD	PR*	HUD	UD	T	D	HD	Yield*	HUD	UD	T	D	HD	PCC*	Fl*	GS*	TF*
99% Purity Constraint																					
1	4●	7	10	13	16	4.24	80	84.5●	89	93.5	98	85.09	0.2●	0.4	0.6	0.8	1.0	0.2	1.47	3.4	5.27
2	4●	7	10	13	16	5.3	65	68	●71	74	77	70.62	0.2●	0.4	0.6	0.8	1.0	0.2	1.98	3.83	5.87
3	5	●8	11	13	16	7.43	65	68	●71	74	77	70.78	0.1●	0.2	0.3	0.4	0.5	0.13	2.63	2.26	6.2
4	5	●8	11	13	16	7.59	50	54	●58	62	66	57.45	0.1	●0.2	0.3	0.4	0.5	0.17	2.84	2.67	7.22
5	8	10●	12	14	16	10.89	50	54	58●	62	66	59.22	0.05	0.1●	0.15	0.2	0.25	0.11	3.96	1.52	7.23
6	10	12●	14	16	18	12.20	50	54	58●	62	66	58.4	0.05	●0.1	0.15	0.2	0.25	0.096	4.43	1.29	7.35
7	2●	4	6	8	10	2.62	80	84.5●	89	93.5	98	85.2	0.2	●0.4	0.6	0.8	1.0	0.33	0.97	6.54	4.91
8	1	2	●3	4	5	2.99	80	84.5	89	93.5	●98	97.05	0.05	0.1	0.15●	0.2	0.25	0.15	0.94	2.06	5.09
9	2●	4	6	8	10	2.96	75	79.5●	84	88.5	93	80.46	0.2	●0.4	0.6	0.8	1.0	0.32	1.12	6.65	5.08
10	0.4	0.8	1.2	●1.6	2	1.54	50	54	58	62●	66	63.62	0.2	0.4	0.6●	0.8	1.0	0.7	0.72	21.0	5.22
11	0.4	0.8	●1.2	1.6	2	1.02	50	54	58	62●	66	62.23	0.6	0.8	●0.9	1.0	1.1	0.872	0.37	21.0	6.46
95% Purity Constraint																					
1	4	7●	10	13	16	7.0	80	84.5●	89	93.5	98	85.35	0.2	●0.4	0.6	0.8	1.0	0.4	1.77	6.24	7.22
2	5	8●	11	14	17	8.05	75	79.5●	84	88.5	93	80.56	0.2	●0.4	0.6	0.8	1.0	0.40	2.05	6.43	7.58
3	5	8	11●	14	17	11.14	65	68	71	74●	77	74.03	0.1	0.2	0.3●	0.4	0.5	0.31	2.89	4.93	8.28
4	5	8	11	14●	17	14.75	65	68	71	74	●77	76.63	0.05	0.1	0.15	0.2●	0.25	0.21	3.57	2.93	8.37
5	8	11	14	17●	20	17.92	50	54	58	62	●66	65.77	0.05	0.1	0.15	0.2●	0.25	0.21	4.51	3.15	9.37
6	14	17	20●	23	26	20.99	50	54	58	62●	66	63.17	0.05	0.1	0.15	●0.2	0.25	0.17	4.59	2.05	11.2
7	20	23●	26	29	32	23.73	50	54	58	62●	66	62.63	0.05	0.1	●0.15	0.2	0.25	0.12	4.59	1.08	12.8
8	11	●14	17	20	23	13.09	65	68●	71	74	77	68.42	0.3●	0.6	0.9	1.2	1.5	0.3	3.37	4.82	8.83
9	●20	21	22	23	24	13.92	●50	54	58	62	66	41.89	●0.5	0.6	0.7	0.8	0.9	0.4	3.99	7.98	12.93
10	1	3●	5	7	9	3.12	84	88●	92	96	99.5	88.97	0.6	0.7●	0.8	0.9	1.0	0.74	0.75	12.11	7.23
11	1	4	●7	10	13	5.87	50	54	58	●62	66	61.27	0.6	0.7	0.8●	0.9	1.0	0.82	1.74	18.69	8.53
12	4	7	10●	13	16	10.34	84	88	92●	96	99.5	92.72	0.05	0.1	0.15●	0.2	0.25	0.16	2.48	2.12	6.99
13	1	4	●7	10	13	6.61	92	96	98●	99	99.5	98.81	0.05	0.1	0.15●	0.2	0.25	0.15	1.57	1.89	6.66

Note: For a 99% purity constraint system: In Cases 2–6 higher production rate is desired, higher yield is desired in Cases 7–8, and in Cases 9–11 higher product pool concentration is desired. For a 95% purity system: In Cases 2–7 higher production rate is desired; both higher production rate and product pool concentration is desired in Cases 8 and 9; Cases 10–11 have higher desirability for product pool concentration; and higher yield is desired in Cases 12–13.

in Cases 2–6. It can be seen from Cases 1–2 that by increasing the flow rate and gradient slope we can attain an increase in the production rate with a corresponding decrease in the yield at a constant product pool concentration. However, if the preferences of the product pool concentration are decreased, as is done in Case 3, the optimal flow rate is increased and the gradient slope is decreased. To obtain a substantially higher value of the production rate, as is evident in Cases 5 and 6, the preferences of both yield and the product pool concentration have to be decreased significantly. As seen in the 99% purity section of the table, this is attained by increasing both flow rate and feed load, and decreasing the gradient slope. An increase in the yield was the objective of Cases 7 and 8. Case 7 shows that, to attain a high yield without sacrificing the product pool concentration, we need to decrease the flow rate and increase the gradient slope. In Case 8, a simultaneous decrease in the preferences of production rate and product pool concentration and an increase in the preferences of yield are required. In Cases 9–11, the preferentially desired design metric is the product pool concentration. The higher product pool concentration is achieved at a lower flow rate, higher gradient slope, and an optimum feed load.

The results for a 95% purity constraint are given in the bottom section of Table 5. When the same design metric preferences are used (Case 1 in the bottom and top sections of Table 5), a decrease in the purity constraint results in a higher value of the optimal production rate, yield, and product pool concentration. In the 95% purity section of Table 5, Cases 2–7 show that a higher value of the production rate can be achieved by increasing the flow rate, decreasing the gradient slope, and increasing the feed load. This in turn results in decreased values of the yield and product pool concentration. In Cases 8 and 9, both higher production rate and product pool concentration are desired. To attain this, all the design parameters are maintained at relatively higher optimal values. However, to attain the higher pool concentration, the production rate must be decreased. In Cases 10 and 11, a higher product pool concentration is attained by decreasing the flow rate and increasing the gradient slope. This in turn results in reductions in the optimal production rate and yield. A high value of yield is obtained in Cases 12 and 13 at moderate flow rate, feed load, and gradient slopes.

After evaluating these different possible scenarios, the question still remains what conditions would one want to use for this separation. Assuming that a yield of less than 85% is unacceptable, one can examine Cases 1, 10, 12, and 13 in the 95% purity section of Table 5. What these data indicate is that if a lower product pool concentration is acceptable, then Case 12 with relatively high values of production rate and yield would be preferred. On the other hand, if a higher product pool concentration is required, then Case 1 would probably be selected because of the low production rate of Case 10. This analysis illustrates the power of the physical programming approach in that it enables the chromatographer to clearly understand the interplay and trade-offs involved in developing optimal processes. Clearly, this could be extended to additional

design metrics (such as economics) to make this approach even more effective.

Conclusions

In this article we have developed a physical programming–based framework for multiobjective optimization and demonstrated that this strategy is well suited to address the priorities and trade-offs of various competing objectives and/or constraints in complex nonlinear chromatographic systems. This approach provides flexibility to the chromatographic engineer and enables the use of physically significant ranges of desirability (such as desirable, tolerable, undesirable, etc.) for each design objective. The presented approach enables visualization and qualitatively evaluates important questions such as: Are the design objectives really conflicting? Is there a reason why one of the design objectives is worse during optimization? Why is one of the objective functions not changing in value? In future work, we will use this approach for multiproduct optimization and for other modes of chromatography (such as step gradient, displacement). In addition, we will use multiobjective optimization in concert with the novel process control method (Nagrath et al., 2003) for improving the performance of large-scale chromatographic processes by reducing batch-to-batch variations.

Acknowledgments

The financial support of Amersham Biosciences is gratefully acknowledged. The authors acknowledge Dr. Karol Lacki from Amersham Biosciences for helpful discussions related to this project.

Literature Cited

Benayoun, R., J. de Montgolfier, J. Tergny, and O. Laritchev, "Linear Programming with Multiple Objective Functions: Step Method (STEM)," *Math. Prog.*, **1**, 366 (1971).

Clark, P. A., and A. W. Westerberg, "Optimization for Design Problems Having More than One Objective," *Comput. Chem. Eng.*, **7**, 259 (1983).

Felinger, A., and G. Guiochon, "Optimization of the Experimental Conditions and the Column Design Parameters in Displacement Chromatography," *J. Chromatogr. A*, **609**, 35 (1992).

Felinger, A., and G. Guiochon, " Comparison of Maximum Production Rates and Optimum Operating/Design Parameters in Overloaded Elution and Displacement Chromatography," *Biotechnol. Bioeng.*, **41**, 134 (1993).

Felinger, A., and G. Guiochon, "Optimizing Experimental Conditions for Minimum Production Cost in Preparative Chromatography," *AIChE J.*, **40**, 594 (1994).

Felinger, A., and G. Guiochon, "Optimizing Experimental Conditions in Overloaded Gradient Elution Chromatography," *Biotechnol. Prog.*, **12**, 638 (1996).

Gadam, S., S. Jayaraman, and S. M. Cramer, "Characterization of Non-Linear Adsorption Properties of Dextran-Based Polyelectrolyte Displacers in Ion-Exchange Systems," *J. Chromatogr.*, **630**, 37 (1992).

Gallant, S. R., S. Vunnum, and S. M. Cramer, "Optimization of Preparative Ion-Exchange Chromatography of Proteins: Linear Gradient Separations," *J. Chromatogr. A*, **725**, 295 (1996).

Golshan-Shirazi, S., and G. Guiochon, "Optimization of the Experimental Conditions in Preparative Liquid Chromatography with Touching Bands," *J. Chromatogr.*, **517**, 229 (1990).

Golshan-Shirazi, S., and G. Guiochon, "Combined Effects of Finite Axial Dispersion and Slow Adsorption Desorption Kinetics on Band Profiles in Nonlinear Chromatography," *J. Phys. Chem.*, **95**, 6390 (1991).

Hollingdale, S. H., *Methods of Operational Analysis in Newer Uses of Mathematics*, J. Lighthill, ed., Penguin Books, Baltimore, MD (1978).

Hwang, C., S. Pady, and K. Yoon, "Mathematical Programming with Multiple Objectives: A Tutorial," *Comput. Oper. Res.*, **7**, 5 (1980).

Ismail-Yahaya, A., and A. Messac, "Effective Generation of the Pareto Frontier: The Normalized Normal Constraint Method," Proc. of 43rd AIAA/ASME/ASCE/AHS/ASC Structures, Structural Dynamics, and Materials Conf., AIAA-2002-1232 (2002).

Jandera, P., D. Komers, and G. Guiochon, "Optimization of the Recovery Yield and of the Production Rate in Overloaded Gradient-Elution Reversed-Phase Chromatography," *J. Chromatogr. A*, **796**, 115 (1998).

Ko, D., and I. L. Moon, "Multiobjective Optimization of Cyclic Adsorption Processes," *Ind. Eng. Chem. Res.*, **41**, 93 (2002).

Luo, R. G., and J. T. Hsu, "Optimization of Gradient Profiles in Ion-Exchange Chromatography for Protein Purification," *Ind. Eng. Chem. Res.*, **36**, 444 (1997).

Messac, A., "Physical Programming: Effective Optimization for Computational Design," *AIAA J.*, **34**, 149 (1996).

Messac, A., "From the Dubious Art of Constructing Objective Functions to the Application of Physical Programming," *AIAA J.*, **38**, 155 (2000).

Messac, A., and X. Chen, "Visualizing the Optimization Process in Real-Time Using Physical Programming," *Eng. Optimiz.*, **32**, 721 (2000).

Messac, A., S. M. Gupta, and B. Akbulut, "Linear Physical Programming: Effective Optimization for Complex Linear Systems," *Trans. Oper. Res.*, **8**, 39 (1996).

Messac, A., J. G. Sundararaj, R. V. Tappeta, and J. E. Renaud, "Ability of Objective Functions to Generate Points on Non-Convex Pareto Frontiers," *AIAA J.*, **38**, 1084 (2000).

Nagrath, D., B. W. Bequette, and S. M. Cramer, "Evolutionary Operation and Control of Chromatographic Processes," *AIChE J.*, **49**, 82 (2003).

Nagrath, D., A. Messac, B. W. Bequette, and S. M. Cramer, "A Hybrid Model Framework for the Optimization of Preparative Chromatographic Processes," *Biotechnol. Prog.*, **20**(1), 162 (2004).

Natarajan, V., B. W. Bequette, and S. M. Cramer, "Optimization of Ion-Exchange Displacement Separations I. Validation of an Iterative Scheme and Its Use as a Methods Development Tool.," *J. Chromatogr. A*, **876**, 51 (2000a).

Natarajan, V., and S. M. Cramer, "A Methodology for the Characterization of Ion-Exchange Resins," *Sep. Sci. Technol.*, **35**, 1719 (2000b).

Natarajan, V., S. Ghose, and S. M. Cramer, "Comparison of Linear Gradient and Displacement Separations in Ion-Exchange Systems," *Biotechnol. Bioeng.*, **78**, 365 (2002).

Tamiz, M., D. Jones, and C. Romero, "Goal Programming for Decision Making: An Overview of the Current State-of-the-Art," *Eur. J. Oper. Res.*, **111**, 569 (1998).

Tseng, C. H., and T. W. Lu, "Minimax Multiobjective Optimization in Structural Design," *Int. J. Numer. Meth. Eng.*, **30**, 1213 (1990).

Manuscript received Feb. 5, 2003, and revision received Jun. 4, 2004.